

SFGNET: SEMANTIC AND FREQUENCY GUIDED NETWORK FOR CAMOUFLAGED OBJECT DETECTION

Dezhen Wang¹, Haixiang Zhao¹, Xiang Shen², Sheng Miao^{1,*}

¹Qingdao University of Technology, Qingdao, Shandong, China

²The George Washington University, Washington, DC, USA

ABSTRACT

Camouflaged object detection (COD) aims to segment objects that blend into their surroundings. However, most existing studies overlook the semantic differences among textual prompts of different targets as well as fine-grained frequency features. In this work, we propose a novel Semantic and Frequency Guided Network (SFGNet), which incorporates semantic prompts and frequency-domain features to capture camouflaged objects and improve boundary perception. We further design Multi-Band Fourier Module(MBFM) to enhance the ability of the network in handling complex backgrounds and blurred boundaries. In addition, we design an Interactive Structure Enhancement Block (ISEB) to ensure structural integrity and boundary details in the predictions. Extensive experiments conducted on three COD benchmark datasets demonstrate that our method significantly outperforms state-of-the-art approaches. The code will be released once the paper is accepted.

Index Terms— Camouflaged object detection, semantic guidance, frequency-domain features, vision-language

1. INTRODUCTION

In nature, many animals and plants blend into their surroundings by altering their color, shape, or other features to avoid predators, a survival strategy known as camouflage [1, 2]. Camouflaged object detection (COD) aims to segment these concealed objects. COD is essential for various applications, including medical image segmentation [2], industrial defect detection [3], and agricultural pest monitoring [4]. CNN-based COD has achieved remarkable progress. However, these methods primarily capture local features while struggling with global contextual dependencies and often neglect fine-grained frequency-domain features, making detection in complex backgrounds challenging. To address these challenges, Cong et al. adopted a two-stage model for coarse localization and detail refinement [5]; Yin et al. introduced masked separable attention with PVT backbone to effectively model global dependencies [6]; Lou et al. proposed VSCode

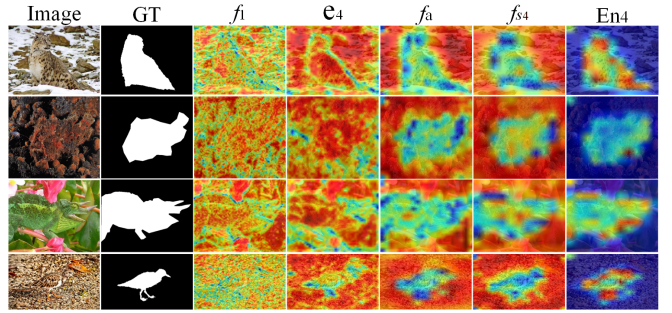


Fig. 1. Visualization of different intermediate feature perceptions in SFGNet.

[7] to improve segmentation performance under complex backgrounds; and Zhang et al. applied class-guided COD to enhance accuracy [8]. Although camouflaged objects resemble their environment in shape, color, and texture, they preserve significant semantic differences across categories. However, existing prompt-based methods fail to fully exploit the relationship between camouflaged objects and their background, and most studies overlook fine-grained frequency-domain features, leading to poor performance in scenarios with cluttered backgrounds, blurred boundaries, or multiple targets.

To address these challenges, we propose a novel Semantic and Frequency Guided Network (SFGNet), which enhances segmentation accuracy by integrating prompts that capture the relationship between camouflaged objects and their background with multi-band frequency representations. Fig. 1 illustrates the intermediate feature representations of SFGNet. Specifically, we first integrate visual features and textual semantics through cross-modal interaction to enhance high-level semantic perception of camouflaged objects. Second, we introduce multi-band frequency modeling and frequency-spatial fusion to better capture fine-grained structures and boundaries. Finally, we design a novel Interactive Structure Enhancement Block (ISEB) to further improve the overall consistency and precision of predictions. The main contributions are summarized as follows:

- We introduce prompts that explicitly model the rela-

*Sheng Miao is the corresponding author.

Emails of each author: 202323050920@stu.qut.edu.cn,
202523051002@stu.qut.edu.cn, xiangshen@gwu.edu, smiao@qut.edu.cn

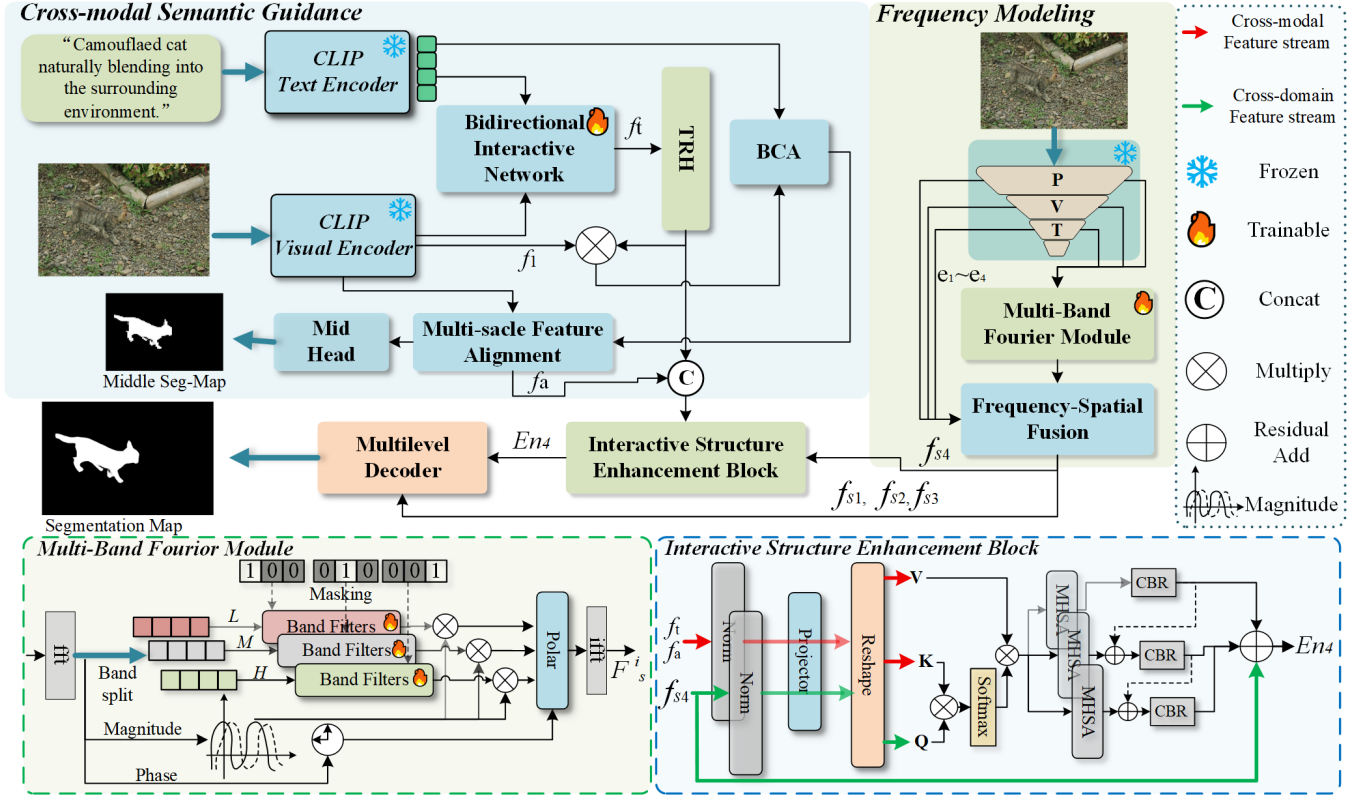


Fig. 2. Overall framework of SFGNet, which leverages textual semantics and frequency-domain features to guide the representation and segmentation of camouflaged objects.

tionship between the target and the background, which effectively enhance the robustness of segmentation.

- We incorporate multi-band frequency feature guidance to capture structural information across low, mid, and high frequencies, improving modeling of complex backgrounds and unclear boundaries.
- We design cross-modal semantic interaction and structure enhancement modules, enabling effective fusion of semantic and visual features while ensuring structural integrity and boundary accuracy.

2. METHODOLOGY

2.1. Overview

Fig. 2 illustrates the overall framework of the proposed Semantic and Frequency Guided Network (SFGNet), which consists of Cross-modal Semantic Guidance and Frequency Modeling, where CLIP extracts semantic representations and the Pyramid Vision Transformer (PVT) provides multi-scale spatial features. The cross-modal features are enhanced via the Bidirectional Interaction Network (BIN), Bidirectional Cross-Attention (BCA), and Multi-Scale Feature Alignment (MFA), while the Multi-Band Fourier Module (MBFM) and Frequency-Spatial Fusion (FSF) integrate frequency- and spatial-domain information. Finally, the Interactive Structure

Enhancement Block (ISEB) and a decoder progressively refine fused features to reconstruct accurate camouflaged object segmentation maps.

2.2. Cross-modal Semantic Guidance

The Cross-modal Semantic Guidance (CSG) module consists of the Bidirectional Interaction Network (BIN), Bidirectional Cross-Attention (BCA), and Multi-Scale Feature Alignment (MFA), which jointly achieve multi-scale interaction and cross-modal fusion. In BIN, the text feature t generates gating coefficients to modulate multi-scale visual features v_3, v_4, v_5 , as shown in Eq. 1.

$$\hat{t} = \sigma(W_g t), \quad \hat{v}_i = W_i v_i \odot \hat{t}_i, \quad i \in \{3, 4, 5\}, \quad (1)$$

BIN further refines features via top-down propagation and bottom-up feedback, as expressed in Eq. 2.

$$\begin{aligned} p_i &= f(\hat{v}_i + \text{Up}(p_{i+1})), \\ n_{i+1} &= f(p_{i+1} + \text{Down}(n_i)), \quad i \in \{3, 4\}, \end{aligned} \quad (2)$$

The Bidirectional Cross-Attention (BCA) module strengthens cross-modal interaction by combining text-guided visual features and visual-guided textual features, as formulated in Eq. 3.

$$F_{\text{BCA}} = \alpha \cdot \hat{X}_t + \beta \cdot \text{Expand}(\hat{T}_x), \quad (3)$$

The Multi-Scale Feature Alignment (MFA) module aligns visual features across scales to reduce semantic inconsistency, with the aligned representation given in Eq. 4.

$$F_{\text{MFA}} = W_f [F'_1 \parallel F'_2 \parallel F'_3], \quad (4)$$

Here, \parallel denotes channel concatenation and W_f is a projection layer. Together, BIN, BCA, and MFA provide consistent and semantically enriched multi-scale features for subsequent modules.

2.3. Frequency Modeling

The Multi-Band Fourier Module (MBFM) enhances feature representation by mapping features into the frequency domain and decomposing them into multiple bands through a masking mechanism, as defined in Eq. 5.

$$\tilde{M}_i(u, v) = \begin{cases} M(u, v), & (u, v) \in \text{band}_i, \\ 0, & \text{otherwise,} \end{cases} \quad (5)$$

Each band-specific component is fused with its phase and transformed back via inverse FFT, as shown in Eq. 6.

$$X_i = F^{-1}(\tilde{M}_i e^{jP}), \quad (6)$$

Finally, all band-specific features are concatenated and projected to yield the frequency-enhanced representation F_{freq} . The Frequency-Spatial Fusion (FSF) module further integrates frequency- and spatial-domain features through complementary attention mechanisms. Channel attention is applied to spatial features, while average and max pooling on frequency features generate a spatial attention map, as formulated in Eq. 7.

$$\begin{aligned} F_c &= F_{\text{spa}} \cdot \sigma(W_c(\text{GAP}(F_{\text{spa}}))), \\ F_s &= F_{\text{freq}} \cdot \sigma(f_s([\text{Avg}(F_{\text{freq}}), \text{Max}(F_{\text{freq}})])), \end{aligned} \quad (7)$$

Here, $\sigma(\cdot)$ is the Sigmoid function and $[\cdot]$ indicates concatenation. The two branches are then merged to obtain the fused representation, as shown in Eq. 8.

$$F_{fs} = \phi([F_c \parallel F_s]), \quad (8)$$

2.4. Interactive Structure Enhancement

The Interactive Structure Enhancement Block (ISEB) refines deep features by attending to auxiliary features, enabling more consistent structures and clearer boundaries, as formulated in Eq. 9.

$$\hat{F} = \text{Softmax}\left(\frac{QK^T}{\sqrt{d}}\right)V, \quad (9)$$

Here, d is the channel scaling factor, and the output \hat{F} is fused with the main feature through a residual connection.

2.5. Loss Function

To jointly ensure pixel-wise accuracy, regional consistency, and cross-modal alignment, we adopt a composite loss consisting of Weighted BCE, Weighted IoU, and Cosine Similarity, as summarized in Eq. 10.

$$L = L_{\text{wBCE}} + L_{\text{wIoU}} + \lambda L_{\text{cos}}, \quad (10)$$

3. EXPERIMENTS AND RESULTS

3.1. Experiments

3.1.1. Datasets

Our experiments were conducted on three publicly available datasets: CAMO [9], COD10K [10], and NC4K [11]. Following the standard training protocol, the training set consists of 1,000 images from CAMO and 3,040 images from COD10K, resulting in a total of 4,040 training images. The test set includes 250 images from CAMO, 2,026 from COD10K, and 4,121 from NC4K, yielding 6,397 images in total for evaluation.

3.1.2. Evaluation Metrics

We employed four widely used metrics to evaluate performance, including the S-measure (S_m) [12], the weighted F-measure (F_β^ω) [13], the mean absolute error (MAE), and the E-measure (E_m) [14].

3.1.3. Implementation Details

To reduce computational cost and leverage the pretrained knowledge of CLIP (ViT-L/336) [15] and PVT (v2-b5), we kept the CLIP and PVT models frozen during training, while the parameters of other network components were learnable. We used AdamW to optimize the network parameters with a learning rate of 0.0001, a batch size of 12, and a total of 200 epochs. Various data augmentation strategies were applied to the training images, including random cropping, horizontal flipping, and color jittering. All experiments were conducted on an NVIDIA RTX 3090 GPU(24 GB memory).

3.2. Comparison with State-of-the-art Methods

We compared SFGNet with several recent and representative methods, including PFNet [16], ZoomNet [17], FSPNet [18], FEDER [19], HitNet [20], FSEL [21], CamoFormer [6], FHCNet [22], VSCode [7], and CGCOD [8]. To ensure fair comparison, all prediction maps were either provided by the original authors or generated using the released codes. Table 1 reports the quantitative comparison between SFGNet and other models. Specifically, SFGNet outperforms the compared methods on CAMO, and NC4K datasets, while achieving comparable performance with CGCOD on COD10K. Qualitative comparisons are illustrated in Figure 3, which demonstrate that SFGNet performs better than state-of-the-art approaches in most cases, and is comparable in a few challenging scenarios. In addition, we evaluated different PVT backbones and found that pvt-v2-b5 achieves the best performance.

3.3. Ablation Studies

To evaluate the effectiveness of key components, we performed ablation studies on the NC4K dataset (4,121 images), as shown in Table 2. The modules (BIN, MFA, ISEB, MBFM, and FSF) were progressively added to the baseline, yielding step-by-step performance gains and confirming the individual

Table 1. Comparative experimental results of LMSGNet and state-of-the-art (SOTA) models on the CAMO, COD10K, and NC4K datasets. The best and second-best values in each column are denoted by bold and underline, respectively.

Methods	Prompt	Backbone	CAMO (250 images)				COD10K (2,026 images)				NC4K (4,121 images)			
			$S_m \uparrow$	$F_\beta^\omega \uparrow$	MAE \downarrow	$E_m \uparrow$	$S_m \uparrow$	$F_\beta^\omega \uparrow$	MAE \downarrow	$E_m \uparrow$	$S_m \uparrow$	$F_\beta^\omega \uparrow$	MAE \downarrow	$E_m \uparrow$
PFNet [16]	None	ResNet	0.782	0.695	0.085	0.855	0.800	0.660	0.040	0.877	0.829	0.745	0.053	0.887
ZoomNet [17]	None	ResNet	0.820	0.752	0.066	0.877	0.838	0.729	0.029	0.888	0.853	0.784	0.043	0.896
FSPNet [18]	None	ViT	0.851	0.802	0.056	0.905	0.850	0.755	0.028	0.912	0.879	0.816	0.035	0.914
FEDER [19]	None	Res2Net	0.836	0.807	0.066	0.897	0.844	0.748	0.029	0.911	0.862	0.824	0.042	0.913
HitNet [20]	None	PVT	0.849	0.809	0.055	0.906	0.871	0.806	0.023	0.935	0.875	0.834	0.037	0.926
FSEL [21]	None	PVT	0.885	0.857	0.040	0.942	0.877	0.799	0.021	0.937	0.892	0.852	0.030	0.941
CamoFormer [6]	None	PVT	0.872	0.831	0.046	0.929	0.869	0.786	0.023	0.932	0.892	0.847	0.030	0.939
FHCNet [22]	None	Swin+Res2Net	0.885	0.842	0.039	0.934	0.869	0.778	0.023	0.931	0.893	0.843	0.031	0.937
VSCode [7]	2D Prompt	Swin	0.873	0.820	0.046	0.925	0.869	0.780	0.025	0.931	0.882	0.841	0.032	0.935
CGCOD [8]	Camoclass	CLIP+PVT	0.896	0.874	0.036	0.947	0.890	0.824	0.018	0.948	0.904	0.879	0.026	0.949
SFGNet	Semantics	CLIP+PVTv2-b2	0.904	0.878	0.034	0.949	0.890	0.826	0.019	0.947	0.907	0.879	0.025	0.952
SFGNet	Semantics	CLIP+PVTv2-b4	0.906	0.879	0.033	0.949	0.890	0.827	0.018	0.948	0.909	0.881	0.023	0.955
SFGNet(Ours)	Semantics	CLIP+PVTv2-b5	0.906	0.880	0.032	0.951	0.891	0.829	0.018	0.949	0.912	0.884	0.021	0.957

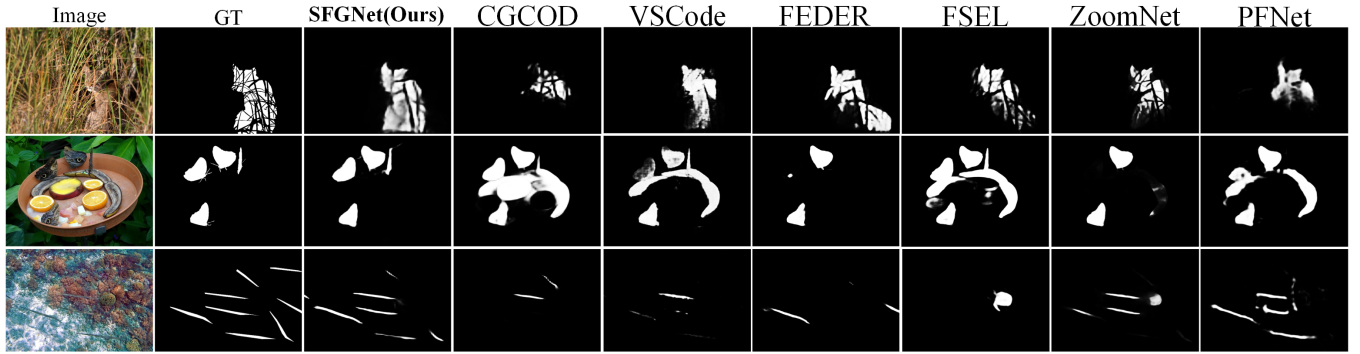


Fig. 3. Comparison of prediction results with state-of-the-art methods. SFGNet outperforms existing approaches in most cases.

Table 2. Ablation study of different components.

Method	NC4K (4,121 images)			
	$S_m \uparrow$	$F_\beta^\omega \uparrow$	MAE \downarrow	$E_m \uparrow$
Base	0.877	0.850	0.031	0.928
+BIN	0.876	0.852	0.032	0.929
+BIN+MFA	0.880	0.859	0.030	0.931
+BIN+MFA+ISEB	0.898	0.872	0.029	0.939
+BIN+MFA+MBFM	0.902	0.876	0.029	0.945
+BIN+MFA+MBFM+FSF	0.907	0.878	0.025	0.952
+BIN+MFA+MBFM+ISEB	0.909	0.880	0.023	0.955
SFGNet (Ours)	0.912	0.884	0.021	0.957

contribution of each. Visualization of intermediate features in Fig. 1 further illustrates the effectiveness of the proposed design.

3.3.1. Analysis of different semantic prompts

To evaluate the impact of different semantic prompts on SFGNet, we recorded the model performance on the COD10K dataset (2,026 images) with various prompts, as summarized in Table 3. The results show that the prompt “Camouflaged $\langle \text{class} \rangle$ naturally blending into the surrounding environment.” achieves the best performance.

Table 3. Impact of different semantic prompts on model performance.

Semantic prompts	COD10K (2,026 images)			
	$S_m \uparrow$	$F_\beta^\omega \uparrow$	MAE \downarrow	$E_m \uparrow$
“A photo of camouflaged object.”	0.881	0.811	0.023	0.940
“A photo of camouflaged $\langle \text{class} \rangle$.”	0.887	<u>0.824</u>	<u>0.019</u>	0.943
“Camouflaged object.”	0.867	0.785	0.027	0.927
“Camouflaged $\langle \text{class} \rangle$.”	0.850	0.755	0.028	0.912
“Camouflaged object naturally blending into the surrounding environment.”	0.888	<u>0.824</u>	<u>0.019</u>	0.946
“Camouflaged $\langle \text{class} \rangle$ naturally blending into the surrounding environment.” (Ours)	0.891	0.829	0.018	0.949

4. CONCLUSION

In this paper, we proposed a Semantic and Frequency Guided Network (SFGNet) for camouflaged object detection. SFGNet integrates cross-modal semantic guidance and multi-band frequency modeling to combine high-level semantics with fine-grained structural cues. Specifically, semantic interaction modules (BIN, BCA, MFA) fuse multi-level visual and textual features, while frequency-domain modeling and spatial fusion (MBFM, FSF) enhance structural and boundary representations. The ISEB further improves result consistency. Extensive experiments show that SFGNet outperforms existing state-of-the-art methods on multiple benchmark datasets.

5. REFERENCES

[1] I. C. Cuthill, M. Stevens, J. Sheppard, T. Maddocks, C. A. Párraga, and T. S. Troscianko, “Disruptive coloration and background pattern matching,” *Nature*, vol. 434, no. 7029, pp. 72–74, 2005.

[2] D. Fan, G. Ji, G. Sun, M. Cheng, J. Shen, and L. Shao, “Camouflaged object detection,” in *2020 IEEE/CVF Conference on Computer Vision and Pattern Recognition (CVPR)*, 2020, pp. 2774–2784.

[3] N. U. Bhajantri and P. Nagabhushan, “Camouflage defect identification: A novel approach,” in *9th International Conference on Information Technology (ICIT’06)*, 2006, pp. 145–148.

[4] D. J. A. Rustia, C. E. Lin, J. Y. Chung, Y. J. Zhuang, J. C. Hsu, and T. T. Lin, “Application of an image and environmental sensor network for automated greenhouse insect pest monitoring,” *Journal of Asia-Pacific Entomology*, vol. 23, no. 1, pp. 17–28, 2020.

[5] R. Cong, M. Sun, S. Zhang, X. Zhou, W. Zhang, and Y. Zhao, “Frequency perception network for camouflaged object detection,” in *Proceedings of the 31st ACM International Conference on Multimedia*, 2023, pp. 1179–1189.

[6] B. Yin, X. Zhang, D. Fan, S. Jiao, M. Cheng, L. Van Gool, and Q. Hou, “Camoformer: Masked separable attention for camouflaged object detection,” *IEEE Transactions on Pattern Analysis and Machine Intelligence*, 2024.

[7] Z. Luo, N. Liu, W. Zhao, X. Yang, D. Zhang, D. Fan, F. Khan, and J. Han, “Vscode: General visual salient and camouflaged object detection with 2d prompt learning,” in *Proceedings of the IEEE/CVF Conference on Computer Vision and Pattern Recognition (CVPR)*, 2023, pp. 17169–17180.

[8] C. Zhang, Q. Zhang, J. Wu, and Y. Pang, “Cgcod: Class-guided camouflaged object detection,” *arXiv preprint arXiv:2412.18977*, 2024.

[9] T. N. Le, T. V. Nguyen, Z. Nie, M. T. Tran, and A. Sugimoto, “Anabranch network for camouflaged object segmentation,” *Computer Vision and Image Understanding*, vol. 184, pp. 45–56, 2019.

[10] D. Fan, G. Ji, M. Cheng, and L. Shao, “Concealed object detection,” *IEEE Transactions on Pattern Analysis and Machine Intelligence*, vol. 44, no. 10, pp. 6024–6042, 2021.

[11] Y. Lv, J. Zhang, Y. Dai, A. Li, B. Liu, N. Barnes, and D. Fan, “Simultaneously localize, segment and rank the camouflaged objects,” in *Proceedings of the IEEE/CVF Conference on Computer Vision and Pattern Recognition (CVPR)*, 2021, pp. 11591–11601.

[12] D. Fan, M. Cheng, Y. Liu, T. Li, and A. Borji, “Structure-measure: A new way to evaluate foreground maps,” in *Proceedings of the IEEE International Conference on Computer Vision (ICCV)*, 2017, pp. 4548–4557.

[13] R. Margolin, L. Zelnik-Manor, and A. Tal, “How to evaluate foreground maps,” in *2014 IEEE Conference on Computer Vision and Pattern Recognition (CVPR)*, 2014, pp. 248–255.

[14] D. Fan, C. Gong, Y. Cao, B. Ren, M. Cheng, and A. Borji, “Enhanced-alignment measure for binary foreground map evaluation,” in *Proceedings of the 27th International Joint Conference on Artificial Intelligence*. 2018, IJCAI’18, p. 698–704, AAAI Press.

[15] M. Xu, Z. Zhang, F. Wei, H. Hu, and X. Bai, “San: Side adapter network for open-vocabulary semantic segmentation,” *IEEE Transactions on Pattern Analysis and Machine Intelligence*, vol. 45, no. 12, pp. 15546–15561, 2023.

[16] H. Mei, G. Ji, Z. Wei, X. Yang, X. Wei, and D. Fan, “Camouflaged object segmentation with distraction mining,” in *Proceedings of the IEEE/CVF Conference on Computer Vision and Pattern Recognition (CVPR)*, 2021, pp. 8772–8781.

[17] Y. Pang, X. Zhao, T. Xiang, L. Zhang, and H. Lu, “Zoom in and out: A mixed-scale triplet network for camouflaged object detection,” in *Proceedings of the IEEE/CVF Conference on Computer Vision and Pattern Recognition (CVPR)*, 2020, pp. 2160–2170.

[18] Z. Huang, H. Dai, T. Xiang, S. Wang, H. Chen, J. Qin, and H. Xiong, “Feature shrinkage pyramid for camouflaged object detection with transformers,” in *2023 IEEE/CVF Conference on Computer Vision and Pattern Recognition (CVPR)*, 2023, pp. 5557–5566.

[19] C. He, K. Li, Y. Zhang, L. Tang, Y. Zhang, Z. Guo, and X. Li, “Camouflaged object detection with feature decomposition and edge reconstruction,” in *2023 IEEE/CVF Conference on Computer Vision and Pattern Recognition (CVPR)*, 2023, pp. 22046–22055.

[20] X. Hu, S. Wang, X. Qin, H. Dai, W. Ren, D. Luo, Y. Tai, and L. Shao, “High-resolution iterative feedback network for camouflaged object detection,” in *Proceedings of the AAAI Conference on Artificial Intelligence*, 2023, vol. 37, pp. 881–889.

[21] Y. Sun, C. Xu, J. Yang, H. Xuan, and L. Luo, “Frequency-spatial entanglement learning for camouflaged object detection,” in *European Conference on Computer Vision (ECCV)*. 2022, pp. 343–360, Springer.

[22] Y. Zhao, Q. Zhang, and Y. Li, “Camouflaged object detection with cnn-transformer harmonization and calibration,” in *ICASSP 2025 IEEE International Conference on Acoustics, Speech and Signal Processing (ICASSP)*. 2025, pp. 1–5, IEEE.